# Empirical and physically based flow rules relevant to high speed processing of 304L steel

O. Lurdos[1], F. Montheillet[1], G. Damamme[2]

[1]*Ecole Nationale Supérieure des Mines de Saint-Étienne, Centre SMS, CNRS UMR 5146*
*158 Cours Fauriel, 42023 Saint-Étienne, Cédex 2, France*
*URL: www.emse.fr* *e-mail: montheil@emse.fr; lurdos@emse.fr*

[2] *CEA-DAM, Centre Île de France, BP 12, 91680 Bruyères-le-châtel, France*
*URL: www.cea.fr* *e-mail: gilles.damamme@cea.fr*

ABSTRACT: Thermomechanical processing of metals involves severe plastic deformation at strain rates up to $10^4$ $s^{-1}$, and temperatures up to the melting point. On the other hand, areas far from the tools may be much less or not affected by strain or temperature. A constitutive equation valid for quasi-static to $10^4$-$10^5$ $s^{-1}$, for temperatures ranging from room temperature to the melting point, and up to strains about 10 is required to predict accurate results. To fit the experimental data, the proposed models tend to a steady state limit with increasing strain, whereas this fundamental characteristic is not reproduced by the most used Johnson-Cook model. Moreover, two distinct types of behaviour are observed according to whether dynamic recrystallization occurs or not. A first empirical model derived from the classical Voce equation is proposed. The second model is physically based on the mechanisms involved during discontinuous dynamic recrystallization. Coefficients are fitted for the case of 304L stainless steel.

Key words: Flow rule, High strain rate, Recrystallization, Stainless steel

## 1 INTRODUCTION

Thermomechanical processing of metals, such as high speed machining or adiabatic cutting involves extreme strains, high strain rates, and intense self-heating. Localization of deformation often leads to the formation of shear bands. Inside shear bands, or more generally in the areas close to processing tools, the plastic strain can be as high as 10, the strain rate is $10^3$-$10^4$ $s^{-1}$, and the temperature rise about 700 to 800°C. On the other hand, the rest of the metal is almost not affected by deformation. An accurate constitutive equation over a wide range of temperature, strain rate and temperature is thus required to model such processes. The particular mathematical form of the well-known Johnson-Cook (JC) [1] equation as a product of three factors as well as the low number of parameters involved has made this model the most commonly used for high speed thermomechanical processing of materials in the industry or research. Three factors describe strain hardening, strain rate sensitivity and temperature sensitivity, respectively. However, some experimental stress-strain curves relative to tantalum [2,3] have shown that such uncoupled form for constitutive equations is not valid. In particular, the strain hardening effect is coupled with strain rate. Moreover, the initial work of Johnson and Cook was based on the study of Taylor impact tests. Such a test involves very high strain rates, but low strains. The validity of the JC equation is thus limited to strains less than unity. The extrapolations and predictions to larger strains are not valid. For the case of 304L stainless steel, Xue et al. [4] have determined the value of the coefficients: A=110 MPa, B=150 MPa, n=0.36, C=1.4, and m=1. This set of parameters applied to an element of material undergoing adiabatic shearing leads to an initial stress equal to 110 MPa. The final state of the element is evaluated for a temperature $T=0.8\ T_m$, a strain $\varepsilon=10$, and a strain rate of $10^4$ $s^{-1}$. According to the Johnson-Cook equation, the final stress is then 1260 MPa. This value that estimates the internal stress inside an adiabatic shear band is over-estimated compared to experimental split Hopkinson pressure bar measurements [5] that give a stress around 1000 MPa at room temperature and 4800 $s^{-1}$. In addition, the intense heating inside the shear band should decrease this stress by a factor 2 to 3.

Moreover, the physical understanding of high speed machining has more and more importance. Indeed, the final microstructure of a deformed metal workpiece has a direct influence on its mechanical properties. The evolutions of the average grain size, deformation texture or dislocation densities are relevant information for industrial engineers. One particular aspect of high strain rate deformation of

metals is the large amount of energy involved during a very short time. Most of it is converted into heat. The Taylor-Quinney parameter, generally of the order of 0.9, measures the fraction of plastic deformation converted into heat. The ten percent remaining are absorbed by the microstructure, whose characteristics evolve under the action of deformation. A particular change is dynamic recrystallization (RX), which has been observed in the case of high speed deformation during adiabatic shearing [6,7] or shaped charge regime [8-10]. Meyers et al. [6,7] observed adiabatic shear bands in austenitic steels with EBSD and TEM. The microstructure inside the shear band is smaller than the resolution of EBSD, but the TEM characterizations show two zones. The first one is composed of well distinct equiaxed grains of size around 100-200 nm. Grain boundaries clearly separate the different grains. The second area is a glassy region. Other experimental observations in the shaped charge regime [8-10] have shown that dynamic RX occurs during jet elongation. Furthermore, the evolution of microstructure is fundamental for the stability of the latter. Murr et al. observed the initial and final microstructures of the charge liner cone.

The above studies both suggest that the crystalline structure was generated by a mechanism of dynamic recrystallization. Derby [11] distinguished two kinds of mechanism for dynamic RX. The first type of behaviour is referred to as continuous dynamic recrystallization (CDRX), and concerns high stacking fault energy materials. A model of CDRX has been proposed by Montheillet et al. [12]. On the other hand, low stacking fault energy materials exhibit a mechanism of discontinuous dynamic recrystallization (DDRX). A model of DDRX was also proposed by Montheillet et al. [13, 14]. Both these mechanisms directly influence microstructure, and as a consequence, flow stress. RX generally occurs during hot working of metals, at low strain rate. The flow stress then goes through a hardening stage followed by softening leading to a steady state stress. A peak stress then occurs. According to such a constitutive behaviour, the stress inside a shear band is lower than outside. Moreover, this peak stress is amplified by self-heating associated with plastic deformation. Figure 1 represents a qualitative description of the stress and strain distributions across a shear band. The difference between the peak stress and the stress inside the band is likely to be at the origin of the band initiation.

The JC constitutive equation does not estimate the qualitative above-mentioned difference since hardening is described by an increasing function that diverges to infinity with strain. The present article

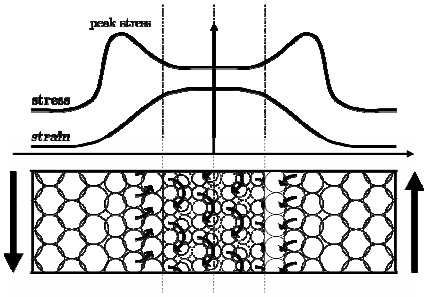


Fig. 1. Schematic representation of a shear band, and qualitative representation of the stress and strain across the band

proposes two alternative models to the JC one. The first one is empirically based on the Voce equation. The second one relies on a physical basis, and proposes a constitutive equation involving DDRX.

## 2 EMPIRICAL CONSTITUTIVE EQUATION

### *2.1 Basic equation*

The classical Voce constitutive equation [15] was first used to describe uniaxial mechanical tests. The flow stress grows from the initial yield stress $\sigma_0$ to a steady state stress $\sigma_S$. However, the fundamental difference with the Johnson-Cook equation is the occurrence of a steady state behaviour in the Voce equation compared to a divergent behaviour of the strain hardening term $A+B\varepsilon^n$ used in the JC equation. The peak stress mentioned in section 1 is modelled by the addition of a simple power term:

$$\sigma = \sigma_S + \left(\sigma_0 - \sigma_S + A\varepsilon^n\right)\exp\left(-r\varepsilon\right) \qquad (1)$$

where $A\varepsilon^n$ is the additional term. This equation will be referred to as the peak Voce model in the following. However, this term can be neglected to reduce the number of coefficients if needed. The strain hardening equation (1) then reduces to the Voce equation, and will be referred to as the Voce model. The Voce equation has already been used for modelling high strain rate processing of materials. The peak Voce and Voce equations (1) only describe strain hardening and softening. The strain rate sensitivity, as well as temperature dependences are accounted for by the variations of parameters of (1) with strain rate and temperature:

$$\sigma_0 = \sigma_0^0\, Z^{m_0} \qquad (2a) \qquad \sigma_S = \sigma_S^0\, Z^{m_S} \qquad (2b)$$

$$A = A_0\, Z^{m_A} \qquad (2c) \qquad n = n_0\, Z^{m_n} \qquad (2d)$$

$$r = r_0\, Z^{m_r} \qquad (2e) \qquad Z = \dot{\varepsilon}\exp\left(Q/RT\right) \qquad (2f)$$

where the classical Zener-Hollomon parameter Z establishes an equivalence between strain rate and temperature effects. Higher strain rates are thus equivalent to lower temperatures.

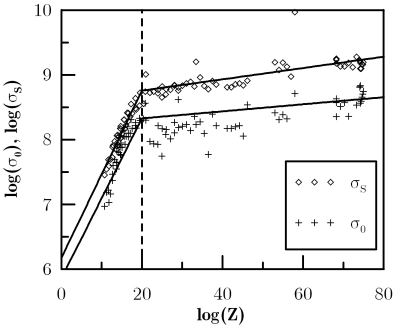


Fig. 2. Experimental data and linear fits for the parameter $\sigma_0$ and $\sigma_s$ of the constitutive equation (1)

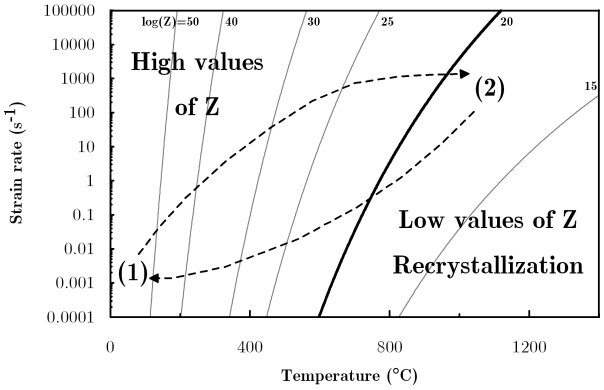


Fig. 3. Diagram showing the limit between the two types of behaviour. Dashed lines represent qualitatively the path followed by a material element inside a shear band. (1) is the initial state, and (2) corresponds to the maximum temperature reached

### *2.2 Identification of the parameters*

Each of the parameters in eq. (1) is completely described by 2 constants: its strain rate sensitivity and its normalization constant. The apparent activation energy Q is then needed to calculate the Zener-Hollomon parameter. The model involves 11 parameters in its complete version or 7 for the simple Voce constitutive equation. A review of experimental stress-strain curves [5, 16-19] was used for the identification. Some scattering of the data is observed, due to the various laboratories, and different testing machines used. However, the large number of experimental data available insures the reliability of the fitted coefficients. Over the 6 sources used, 90 experimental stress-strain curves were available for strain rates ranging from the quasi-static domain to 4800 $s^{-1}$, and temperatures from 20°C to 1150°C. Figure 2 shows double-logarithmic plots of the parameter $\sigma_0$ of the constitutive equation. Two different linear domains appear. The limit between the two zones is log Z=20. Numerical values of the parameters are reported in Table I for each domain.

The occurrence of a peak stress on a stress-strain curve means that the material softens by dynamic recrystallization. 304L stainless steel then undergoes (discontinuous) dynamic recrystallization (RX) only if log Z≤20. For higher values, the experimental stress-strain curves do not exhibit a peak, denoting the absence of RX. Figure 3 shows the area where RX operates for 304L in a temperature-strain rate diagram, and the qualitative path followed by a material element inside a shear band. In the initial state (1), the temperature is the initial, i.e. room temperature and the strain rate is zero. When the chipping tool deforms the workpiece, shear bands appear, and the strain rate and temperature rapidly increase. The melting point is reached for adiabatic shear bands (2). The case of high strain rate processing falls inside or very close to the area of recrystallization.

Table 1. Parameters of the linear fits in Figure 2

| Parameter | log Z ≤ 20 | log Z ≥ 20 |
|---|---|---|
| $\log\sigma_0$ (MPa) = | $5.86+0.123\log Z$ | $8.22+5.45\times10^{-3}\log Z$ |
| $\log\sigma_S$ (MPa) = | $6.18+0.129\log Z$ | $8.58+8.73\times10^{-3}\log Z$ |
| log r = | $1.34-0.0343\log Z$ | $0.725-3.58\times10^{-3}\log Z$ |
| log A (MPa) = | $5.37+0.201\log Z$ | $29.51-1.01\log Z$ |
| log n = | $0.217-0.109\log Z$ | $8.93-0.545\log Z$ |

## 3 PHYSICALLY BASED CONSTITUTIVE EQUATION

304L stainless steel belongs to the low stacking fault energy materials that recrystallize discontinuously. A general model has been proposed by Montheillet et al. [13, 14]. The material is represented by a set of N spherical grains. Each grain is defined by two internal variables: the diameter $D_i$ and the dislocation density $\rho_i$. The evolutions of these physical parameters are described by the following equations:

$$dD_i/dt = 2M\tau(\bar{\rho}-\rho_i) \text{ and } d\rho_i/d\varepsilon = h - r\rho_i \quad (3)$$

where M is the grain boundary mobility, $\tau=\mu b^2$, $\mu$ is the shear modulus and b is the Burgers vector. The strain hardening equation chosen here has been proposed by Yoshie-Lasraoui-Jonas [20, 21] (YLJ). Other strain hardening equations can be substituted to the YLJ one. However, the YLJ equation gives satisfying results and is relevant to hot working of metals [21]. This equation involves two parameters. The first one, h, describes hardening whereas the second, r, is associated with dynamic recovery. At last, $\bar{\rho}$ is the average dislocation density weighted by the grain surface areas to insure incompressibility:

$$\bar{\rho} = \sum_{i=1}^{N}\rho_i D_i^2 \Big/ \sum_{i=1}^{N} D_i^2 \quad (4)$$

The flow stress is then simply derived from the average dislocation density according to $\sigma = \alpha\mu b\sqrt{\bar{\rho}}$. Following the above two evolution equations, the dislocation density increases with strain. The size of grains then increases until its maximum. The dislocation density of the considered grain is then equal to the average dislocation density. Then, the size decreases until the grain vanishes. A third equation is necessary to describe the nucleation of new grains within the matrix. Nucleation is the fundamental characteristic of DDRX, by contrast to continuous dynamic recrystallization. Older hardened grains disappear to the benefit of new dislocation free grains. A general form of the total number of new grains appearing per unit time and volume is chosen to account any physical type of nucleation:

$$\left(dN/dt\right)^{+} = k\bar{\rho}^{p}\sum_{i=1}^{N} D_i^2 \qquad (5)$$

where k is a nucleation constant. The exponent of $\bar{\rho}$ is a constant that does not depend either on temperature or on strain rate, and its value is close to 3 [13, 14]. The four equations (3) to (5) constitute the basis of the model. Parameters h, r, k and M vary with temperature and strain rate according to:

$$\begin{aligned} h &= h_0\dot{\varepsilon}^{m_h}\exp\left(m_h Q_h/RT\right) & k &= k_0\exp\left(-Q_n/RT\right) \\ r &= r_0\dot{\varepsilon}^{-m_r}\exp\left(-m_r Q_r/RT\right) & M &= M_0\exp\left(-Q_M/RT\right) \end{aligned} \qquad (6)$$

and the associated numerical values are given in Table 2. The model is therefore fully defined by 10 parameters, which were fitted with the same experimental stress-strain curves as the previous empirical model (section 2). Full details on the method used to derive the parameters and numerical values are given in [13, 14].

## 4 CONCLUSIONS

The two proposed models represent correctly the behaviour of low stacking fault energy metals for a wide range of temperatures and strain rates. The fundamental difference of the proposed models with the existing ones is the occurrence of a steady state stress when strain becomes very large. This characteristic should be responsible for the apparition of shear bands due to a more intense stress reduction inside severely deformed zones. The parameters were fitted for the case of 304L stainless steel using both models. Two distinct domains appear, according to whether recrystallization occurs or not. The typical values of temperature and strain rate for thermomechanical processing of materials do involve the dynamic recrystallization regime.

Table 2. Parameters of the physically based constitutive equation (R is the gas constant)

| Parameter | $\log Z \le 21$ | $\log Z \ge 21$ |
|---|---|---|
| $\log h\,(\mu m^{-2}) =$ | $0.19 + 0.17\log Z$ | $3.56 + 9.1\times10^{-3}\log Z$ |
| $\log r =$ | $1.39 - 3.69\times10^{-2}\log Z$ | $0.68 - 2.92\times10^{-3}\log Z$ |
| $\log k\,(m^4 s^{-1}) =$ | $3.25 - 137\,(kJ\,mol^{-1})/RT$ | |
| $\log M\tau\,(m^3 s^{-1}) =$ | $5.65 - 69.3\,(kJ\,mol^{-1})/RT$ | |

ACKNOWLEDGEMENTS

This investigation was carried out under financial support of the CETIM Foundation, which is gratefully acknowledged.

REFERENCES

1. G.R. Johnson and Cook W.H., 7th International Symposium on Ballistics, La Hague, The Netherlands, 1983, 541–548.
2. R. Liang and A.S. Khan, *Int J Plast.* 15 (1999) 963-980.
3. A.S. Khan and R. Liang, *Int J Plast.* 15,(1999),1089-1109.
4. Q. Xue, V.F. Nesterenko and M.A. Meyers, *Int J Imp Eng*. 28 (2003) 257-280.
5. W.S. Lee, C.F. Lin, *Mater Sci Engn*. 308 (2001) 124-135
6. M.A. Meyers, Y.B. Xu, Q. Xue, et al., *Acta Mater*. 51 (2003) 1307-1325.
7. M.A. Meyers, V.F. Nesterenko, J.C. La Salvia et al., *J Phys IV*. 10 (2000) 51-56.
8. L.E. Murr, H.K. Shih, C.S. Niou, et al., *Scripta Metall Mater*. 29 (1993) 567-572.
9. L.E. Murr, C.S. Niou, J.C. Sanchez, et al., *Scripta Metall. Mater*. 32 (1995) 31-36.
10. L.E. Murr, C.S. Niou, J.C. Sanchez, et al., *J. Mater. Sci*. 30 (1995) 2747-2758.
11. B. Derby, *Acta Metall Mater*. 39 (1991) 955-962.
12. S. Gourdet and F. Montheillet, *Acta Mater*. 50 (2002) 2801-2812.
13. F. Montheillet, O. Lurdos and G. Damamme, submitted to *Acta Mater*., (2007).
14. O. Lurdos, F. Montheillet and D. Damamme, submitted to *Acta Mater*., (2007).
15. E. Voce. *J Inst Metals*, 74 (1948) 537-562.
16. A. Belyakov, H. Miura and T. Sakai, *Mater Sci Engn*. A255 (1998) 139-147.
17. M. El Wahabi, J.M. Cabrera, J.M. Prado, *Mater Sci. Engn*, A343 (2003) 116-125.
18. S. Venugopal, S.L. Mannan, Y.V.R.K. Prasad, *J. Mater. Proc. Tech*., 65, 1997, 107-115.
19. C. Jovic, Rapport de synthèse : Apport de la dynamique en forgeage à froid, synthese report, CETIM, 2005.
20. A. Yoshie, H. Morikawa, et al., *Trans ISIJ*. 27 (1987) 425-431.
21. A. Lasraoui and J.J. Jonas, *Metal. Trans*., 22A (1991) 1545-1558.